Available online at www.sciencedirect.com
SCIENCE DIRECT®
ELSEVIER
Nuclear Physics A 758 (2005) 619c–626c
NUCLEAR PHYSICS A

New results of presolar-grain studies and constraints on nucleosynthesis and stellar evolution

E. Zinner

Physics Department and Laboratory for Space Sciences,
Washington University, St. Louis, MO 63130, USA

A new type of secondary ion mass spectrometer, the NanoSIMS, allows the elemental and isotopic analysis of smaller samples than could be measured previously. This instrument has been successfully applied to studies of new types of presolar grains in primitive meteorites and interplanetary dust particles (IDPs). Examples include O- and Mg-isotopic measurements of sub-μm spinel grains, the discovery of presolar silicates in IDPs and meteorites, and the Mg- and Ti-isotopic analysis of rare classes of presolar silicon carbide grains.

1. INTRODUCTION

The study of presolar dust grains from primitive meteorites, in particular of their isotopic compositions, has provided a wealth of information with important implications for nucleosynthesis, stellar evolution, galactic chemical evolution, conditions in stellar atmospheres, mixing of supernova ejecta, and physical and chemical conditions in the early solar system and in the parent bodies of the grains' host meteorites [1]. These grains are identified as having a stellar origin by their isotopic compositions, which are completely different from those of solar-system material. Because of the grains' small sizes, the instrument of choice for their isotopic analysis has been the ion microprobe. Since their discovery in 1987, thousands of presolar grains, mostly silicon carbide (SiC), graphite, and corundum (Al_2O_3), have been analyzed with this instrument for their isotopic ratios [2, 3, 4].

Although most presolar dust grains are smaller than 1μm [5], almost all of these measurements had been made on grains 1μm or larger in diameter. Recently, a new type of ion microprobe, the NanoSIMS, has become commercially available [6], and the first instrument was installed at Washington University. The main distinguishing features of this instrument are: 1) because of normal incidence of the primary ion beam, a very small beam spot and thus high spatial resolution are achieved; 2) because of the NanoSIMS's unique ion-optical design, the secondary ion transmission at high mass resolution, necessary for most isotopic measurements, is very high; and 3) the instrument has six detectors, which can be used for simultaneous measurements of secondary ions [7]. The increase in spatial resolution and sensitivity allows the analysis of much smaller presolar grains than has previously been possible. We have exploited this new capability to identify presolar spinel grains and measure their O- and Mg-isotopic ratios, to search for presolar silicates in IDPs and meteorites, and to study rare types of presolar SiC grains that are more abundant among sub-micron grains than among larger ones.

0375-9474/$ – see front matter
doi:10.1016/j.nuclphysa.2005.05.112

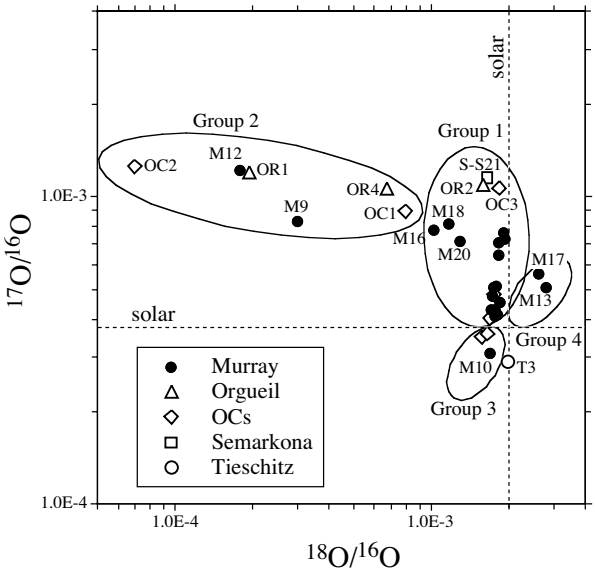

Figure 1. Oxygen-isotopic ratios of presolar spinel grains from the carbonaceous chondrites Murray (CM2), Orgueil (CI), and the ordinary chondrites Semarkona (LL3.0), Tieschitz (H3.6) and a mixture of Semarkona, Bishunpur (LL3.1), and Krymka (LL3.1) (OCs).

2. PRESOLAR SPINEL GRAINS

Up until a couple of years ago, most presolar oxide grains were identified as corundum [8]. Presolar spinel ($MgAl_2O_4$) was believed to be extremely rare, and only a few grains were known. In 1988, Zinner and Tang [9] made O-isotopic measurements of a spinel-rich separate from the Murray carbonaceous meteorite and found ^{17}O excesses. Because the spinel grains in this separate have an average diameter of only 0.15μm, at that time it was not possible to analyze individual grains, and measurements were made on aggregates of hundreds of grains. The NanoSIMS makes it possible to measure the O-isotopic ratios of grains of this size. Such measurements are made on grains deposited on a gold foil from liquid suspension. Candidate grains are identified from raster images in negative ^{16}O secondary ions and secondary electrons. The primary ion beam is then deflected onto selected grains, and isotopic analyses are made in multidetection. Such measurements on hundreds of grains showed that the abundance of presolar spinel grains is ~2.4% among grains of average diameter 0.15μm and ~1.7% among grains of diameter ~0.45μm, whereas the abundance is at least a factor of 20 lower among ≥1μm grains [10, 11].

While 0.15μm-large grains are completely consumed during O-isotopic analysis, enough material remains for other analyses in 0.5μm-large grains. Figures 1 and 2 show the O- and Mg-isotopic ratios of 32 presolar spinel grains [12, 13, 11]. Also shown in Fig. 1 are the four groups defined for presolar corundum grains by Nittler et al. [8].

As has been argued for presolar corundum grains [8], the O-isotopic ratios of the spinel grains indicate an origin in red giant branch (RGB) or asymptotic branch (AGB) stars. Closer inspection of the two figures shows that there is no correlation between the O- and Mg-isotopic ratios of the grains. This observation is not surprising because different

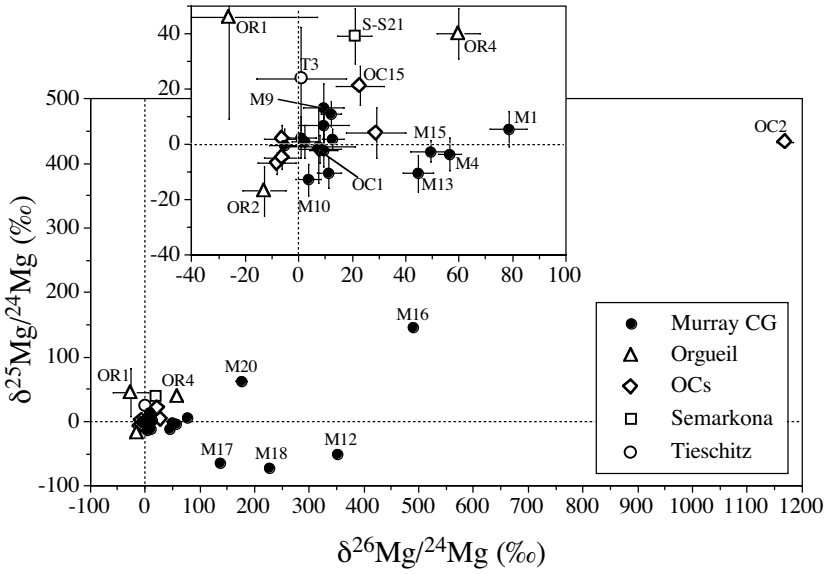

Figure 2. Magnesium isotopic ratios of the presolar spinel grains whose O-isotopic ratios are shown in Fig. 1. The isotopic ratios are plotted as delta values, deviations from the solar-system (terrestrial) ratios (^{25}Mg/^{24}Mg=0.12663 and ^{26}Mg/^{24}Mg=0.13932) in permil.

nuclear processes occurring at different stages of stellar evolution affect the isotopic ratios of these two elements. First dredge-up of material after main-sequence H burning is expected to enrich the star's envelope in ^{17}O and deplete it in ^{18}O [14], and the compositions of Group 1 grains (Fig. 1) are explained in this way. The large ^{18}O depletions of Group 2 grains are explained by invoking extra mixing (also called cool bottom processing or CBP) in low-mass RGB and thermally pulsing (TP) AGB stars [15, 16], possibly also by hot bottom burning (HBB) [17]. In contrast to O, the Mg isotopes are mostly affected by proton-capture reactions in the H-burning shell [18] and α-capture reactions on ^{22}Ne and neutron capture in the He-burning shell [11] during the RGB and AGB phases. Proton capture, also during CBP and HBB, leads mostly to ^{26}Al production with accompanying destruction of ^{25}Mg [18]. Because Al is enriched over Mg in spinel grains by a factor of 20 compared to the stellar envelope, *in situ* decay of ^{26}Al in the grains leads to much larger ^{26}Mg excesses than the ^{25}Mg depletions. For both O and Mg, galactic chemical evolution (GCE) is expected to result in increases of the heavy isotopes ^{17,18}O relative to ^{16}O and ^{25,26}Mg relative to ^{24}Mg with increasing age of the Galaxy [19, 20].

While the Mg-isotopic ratios of the grains in the overlying graph of Fig. 2 can be explained by models of low-mass AGB stars involving He-burning and ^{26}Al production in the H-burning shell [11], the ^{26}Mg excesses in the Murray grains M12, M16-18, and M20, and especially in grain OC2, are much too large to be explained this way. Grain OC2 is probably from an intermediate-mass AGB star that experienced HBB [21]. The Murray

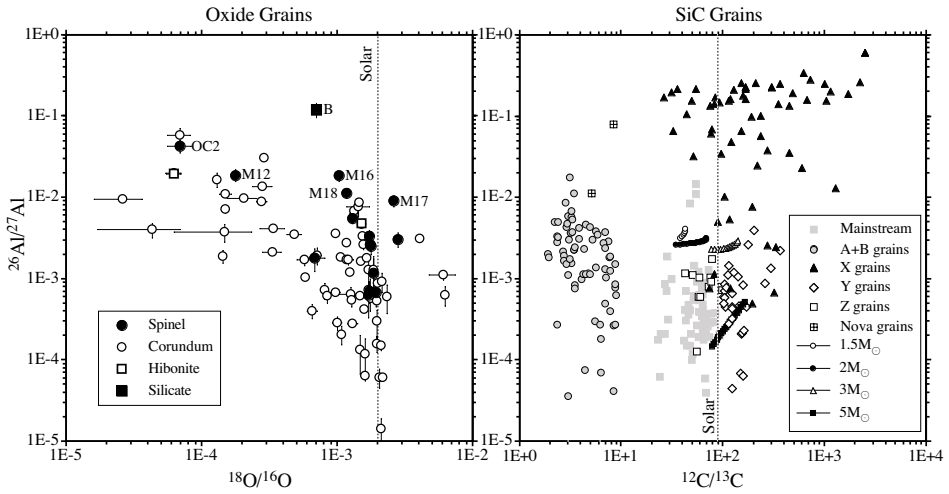

Figure 3. Comparison of inferred $^{26}Al/^{27}Al$ ratios in presolar oxide and SiC grains. The right graph also shows predictions of AGB models for the envelope of TP-AGB stars with C>O for sequential thermal pulses and third dredge-up [11]. SiC data are from [22, 23, 24, 25, 26, 27] and unpublished from Washington University. See section 3 for a discussion of silicate grain B.

grains with large ^{26}Mg excesses are most likely from low-mass AGB stars with CBP. Their ^{25}Mg excesses and deficits can be explained by He burning and/or GCE effects. Nollet et al. [16] have already noticed the large inferred $^{26}Al/^{27}Al$ ratios observed in presolar corundum grains. Their CBP model is based on two parameters: the mass circulation rate affects mostly the $^{18}O/^{16}O$ ratio in the envelope and thus in oxide grains from AGB stars, whereas the temperature experienced by the circulating material determines the $^{26}Al/^{27}Al$ ratio. Temperatures implied by the $^{26}Al/^{27}Al$ ratios inferred for presolar spinel grains range up to ~$50T_6$.

One unexpected observation is that inferred $^{26}Al/^{27}Al$ ratios in presolar oxide grains reach much higher values than ratios in presolar SiC grains from AGB stars (mainstream, Y, and Z grains) (Fig. 3). Figure 3b also shows predictions of AGB models for the $^{12}C/^{13}C$ and $^{26}Al/^{27}Al$ ratios. Only three mainstream grains have $^{26}Al/^{27}Al$ ratios higher than the predictions. The ratios in A+B grains are higher. These and the low $^{12}C/^{13}C$ ratios of these grains must be the result of H burning, but we still do not know in which stellar environment these processes occurred [27]. The $^{26}Al/^{27}Al$ ratios of oxide grains are even higher, reaching into the range of SiC grains from novae and supernovae (the X grains). This is surprising. The $^{17}O/^{16}O$ ratios of presolar oxide grains indicate that they come from low-mass RGB and AGB stars [8], and abundant evidence exists that mainstream SiC grains are from low-mass AGB stars [28]. However, if the mainstream SiC grains formed in the same stars that produced presolar oxide grains before they turned into carbon stars, their $^{26}Al/^{27}Al$ ratios are expected to be at least as high as those of the oxide grains. That this is not the case indicates that the parent stars of oxide grains with high $^{26}Al/^{27}Al$ ratios must be different from those of mainstream SiC grains, and the CBP experienced by the former might have prevented them from becoming carbon stars.

3. PRESOLAR SILICATE GRAINS

The O-isotopic data of spinel grains plotted in Fig. 1 were obtained by single-grain analysis of well separated grains as described above. An alternate method consists of analyzing tightly packed grains by raster imaging. This method has the advantage that thousands of grains can be analyzed for their isotopic compositions in one image. Nguyen et al. [29] used this method successfully to identify 252 presolar spinel and 32 presolar corundum grains in two acid residues from the Murray meteorite with average diameters of 0.15μm and 0.45μm. The disadvantage of this method is that, because the primary ion beam of Cs overlaps onto neighboring isotopically normal grains, some small presolar grains are not detected.

Isotopic raster imaging was key to the discovery of presolar silicates in IDPs [30]. It was applied to fragments of an IDP pressed into a gold foil. As of today, at least 17 presolar silicate grains have been identified in IDPs [30, 31, 32]; their O-isotopic ratios are plotted in Fig. 4. Their abundance might depend on IDP type; the average abundance in all IDPs analyzed so far is ~900ppm, higher than that of any presolar grain species in primitive meteorites [4]. Although astronomical observations indicate the presence of silicate grains in circumstellar dust shells around AGB stars [33, 34], previous searches for presolar silicates in primitive meteorites were unsuccessful [35, 36]. As for IDPs, the high spatial resolution and high sensitivity of the NanoSIMS led to the first identification of presolar silicate grains in primitive meteorites [37, 38]. Their abundance is ~70ppm of the whole meteorite.

Figure 4 shows the O-isotopic ratios of all presolar silicate grains in IDPs [30, 31, 32] and primitive meteorites [39, 40, 38] identified to date. Comparison with Fig. 1 reveals that all four groups are represented, but there are some grains with unusual isotopic compositions. Grain A has an extremely large ^{17}O excess, almost as large as that of a unique corundum grain from Tieschitz [8], but its ^{18}O depletion is not as large. However, grain A was found during isotopic imaging of a polished section of the Acfer 094 meteorite, and contribution from surrounding, isotopically normal, material could have reduced a previously large ^{18}O depletion. Nittler et al. [8] argued that the unique Tieschitz

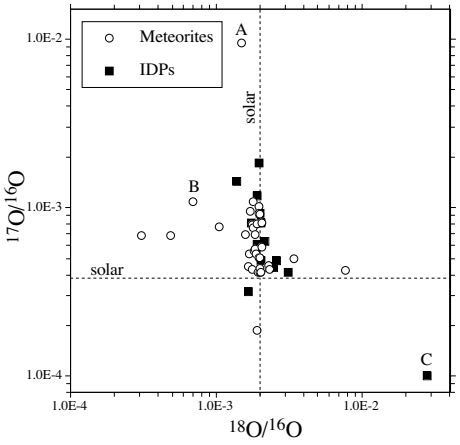

Figure 4. Oxygen-isotopic ratios of presolar silicate grains in primitive meteorites and IDPs. Three interesting grains are labeled and are discussed in the text.

grain originated from an intermediate-mass AGB star that experienced HBB, and it is likely that grain A also came from such a star.

Grain B is the only presolar silicate whose Mg-isotopic ratios were measured and exhibited a ^{26}Mg excess of 120‰. Because the Al/Mg ratio of this grain is not very high, the inferred ^{26}Al/^{27}Al ratio is 0.12, higher than in any presolar oxide grains (see Fig. 3). If CBP is responsible for this high ratio, according to the Nollet et al. [16] model the temperature reached by the circulated material must have been almost $60T_6$. A possibility is that grain B has a SN origin. The He/N layer of a Type II supernova has the basic isotopic signatures of grain B: large ^{17}O excesses, large ^{18}O depletions, and high ^{26}Al/^{27}Al ratios [41]. However, this layer, which experienced H burning in the CNO cycle, has about 50 times more N than O, and it is not clear whether any silicate grains can condense under such conditions.

An oxygen-isotopic composition such as that of grain C has never been seen before. Large ^{18}O excesses have been found in low-density presolar graphite grains and have been attributed to a Type II SN origin [42]. The He/C zone of such supernovae is rich in ^{18}O due to α-capture on ^{14}N. However, this layer has C»O, and mixing with the underlying O-rich layer, consisting mostly of ^{16}O, is necessary to achieve O>C and the elemental and O-isotopic compositions of grain C [32].

4. RARE TYPES OF PRESOLAR SILICON CARBIDE

Different types of presolar SiC have been defined on the basis of the C-, N-, and Si-isotopic compositions of single grains [22, 4]. It was found that the abundances of some rare types such as Y and Z grains increase with decreasing grain size. Application of the NanoSIMS has resulted in the identification of relatively large numbers of these grain types among SiC grains of ~0.5µm diameter and has made it possible to perform Al-Mg and Ti-isotopic analyses on Z grains for the first time. These grains have ^{29}Si depletions and large ^{30}Si excesses and are believed to come from low-metallicity AGB stars [43].

Figure 3 shows inferred ^{26}Al/^{27}Al ratios of Z grains measured with the NanoSIMS. The ratios cover the same range as most mainstream grains, indicating that metallicity has little effect on the production of ^{26}Al in AGB stars. Figure 5 shows isotopic patterns of Si

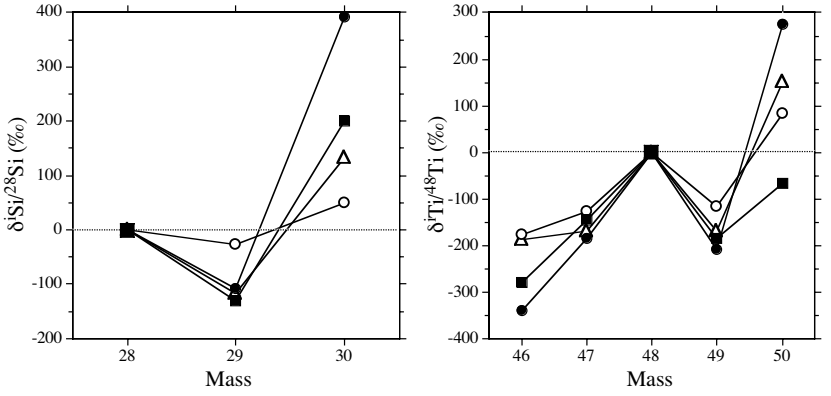

Figure 5. Silicon- and Ti-isotopic patterns of presolar SiC grains of type Z. Ratios are expressed as δ-values, deviations from the solar ratios in permil.

and Ti in selected Z grains. The Si- and Ti-isotopic ratios of mainstream grains are characterized by excesses of ^{29,30}Si relative to ^{28}Si and excesses of all the Ti isotopes relative to ^{48}Ti. These signatures reflect both n-capture in AGB stars and differences in the initial isotopic compositions of these elements in the parent stars due to GCE effects. In contrast, the Z grains show depletions in ^{29}Si and ^{46,47,49}Ti and variable excesses in ^{30}Si and ^{50}Ti. The depletions most likely reflect an origin in low-metallicity stars and the GCE of the Si- and Ti-isotopic ratios. Model calculations indicate that enhancements from n-capture effects are larger in low-metallicity AGB stars than in stars of solar metallicity [44], and for ^{30}Si and ^{50}Ti these enhancements apparently overwhelm the initial depletions in the grains' parent stars. However, there is no simple correlation between the depletions and enhancements in different Si and Ti isotopes.

5. CONCLUSIONS

The capability of the NanoSIMS to analyze small grains with high sensitivity has led to new advances in the study of presolar grains with important astrophysical implications. Among them are:

a) Spinel is a major presolar grain species.
b) Mg-isotopic ratios in presolar spinel grains indicate a prevalence of cool bottom processing.
c) The parent stars of oxide grains with high ^{26}Al/^{27}Al ratios differ fundamentally from the parent stars of mainstream SiC grains.
d) Presolar silicates were discovered in IDPs and primitive meteorites.
e) A unique presolar silicate grain originated from a supernova.
f) The ^{26}Al/^{27}Al ratios of Z SiC grains indicate that metallicity does not have a major effect on the production of ^{26}Al in AGB stars, and the Ti-isotopic ratios agree with a low-metallicity origin of these grains.

REFERENCES

1. T. J. Bernatowicz and E. Zinner (eds.), Astrophysical Implications of the Laboratory Study of Presolar Materials, AIP, New York, 1997.
2. E. Zinner, Ann. Rev. Earth Planet. Sci. 26 (1998) 147.
3. L. R. Nittler, Earth & Planet. Sci. Lett. 209 (2003) 259.
4. E. Zinner, in Treatise on Geochemistry, K. K. Turekian, H. D. Holland and v. e. A. M. Davis, Eds. Elsevier, Oxford and San Diego, vol. 1, p. 17 2004.
5. S. Amari, R. S. Lewis and E. Anders, Geochim. Cosmochim. Acta 58 (1994) 459.
6. F. J. Stadermann, R. M. Walker and E. Zinner, NANOSIMS: A new generation ion probe for the microanalysis of natural materials, Beyond 2000-New Frontiers in Isotope Geoscience, Univ. of Melbourne, Lorne, Australia (2000).
7. G. Slodzian, F. Hillion, F. J. Stadermann and F. Horreard, Applied Surface Sci. 203-204 (2003) 798.
8. L. R. Nittler, C. M. O'D. Alexander, X. Gao, R. M. Walker and E. Zinner, Astrophys. J. 483 (1997) 475.
9. E. Zinner and M. Tang, Lunar Planet. Sci. XIX (1988) 1323.
10. E. Zinner, S. Amari, R. Guinness, A. Nguyen, F. Stadermann, R. M. Walker and R. S. Lewis, Geochim. Cosmochim. Acta 67 (2003) 5083.
11. E. Zinner, L. R. Nittler, P. Hoppe, R. Gallino, O. Straniero and C. M. O'D. Alexander, Geochim. Cosmochim. Acta (2004) submitted.
12. L. R. Nittler, C. M. O'D. Alexander, X. Gao, R. M. Walker and E. K. Zinner, Nature 370 (1994) 443.

13. B.-G. Choi, G. R. Huss, G. J. Wasserburg and R. Gallino, Science 282 (1998) 1284.
14. A. I. Boothroyd and I.-J. Sackmann, Astrophys. J. 510 (1999) 232.
15. G. J. Wasserburg, A. I. Boothroyd and I.-J. Sackmann, Astrophys. J. 447 (1995) L37.
16. K. M. Nollett, M. Busso and G. J. Wasserburg, Astrophys. J. 582 (2003) 1036.
17. A. I. Boothroyd, I.-J. Sackmann and G. J. Wasserburg, Astrophys. J. 442 (1995) L21.
18. A. I. Karakas and J. C. Lattanzio, Pub. Astron. Soc. Australia 20 (2003) 279.
19. F. X. Timmes, S. E. Woosley and T. A. Weaver, Astrophys. J. Suppl. 98 (1995) 617.
20. Y. Fenner, B. K. Gibson, H.-c. Lee, A. I. Karakas, J. C. Lattanzio, A. Chieffi, M. Limongi and D. Yong, Pub. Astron. Soc. Australia 20 (2003) 340.
21. L. R. Nittler, P. Hoppe, C. M. O'D. Alexander, M. Busso, R. Gallino, K. K. Marhas and K. Nollett, Lunar Planet. Sci. XXXIV (2003) Abstract #1703.
22. P. Hoppe, S. Amari, E. Zinner, T. Ireland and R. S. Lewis, Astrophys. J. 430 (1994) 870.
23. L. R. Nittler, P. Hoppe, C. M. O'D. Alexander, S. Amari, P. Eberhardt, X. Gao, R. S. Lewis, R. Strebel, R. M. Walker and E. Zinner, Astrophys. J. 453 (1995) L25.
24. P. Hoppe, R. Strebel, P. Eberhardt, S. Amari and R. S. Lewis, Meteorit. Planet. Sci. 35 (2000) 1157.
25. S. Amari, X. Gao, L. Nittler, E. Zinner, J. José, M. Hernanz and R. Lewis, Astrophys. J. 551 (2001) 1065.
26. S. Amari, L. R. Nittler, E. Zinner, R. Gallino, M. Lugaro and R. S. Lewis, Astrophys. J. 546 (2001) 248.
27. S. Amari, L. R. Nittler, E. Zinner, K. Lodders and R. S. Lewis, Astrophys. J. 559 (2001) 463.
28. M. Lugaro, A. M. Davis, R. Gallino, M. J. Pellin, O. Straniero and F. Käppeler, Astrophys. J. 593 (2003) 486.
29. A. Nguyen, E. Zinner and R. S. Lewis, Publ. Astron. Soc. Australia 20 (2003) 382.
30. S. Messenger, L. P. Keller, F. J. Stadermann, R. M. Walker and E. Zinner, Science 300 (2003) 105.
31. C. Floss and F. J. Stadermann, Lunar Planet. Sci. XXXV (2004) Abstract #1281.
32. S. Messenger and L. P. Keller, Meteorit. Planet. Sci. 39 (2004) submitted.
33. L. B. F. M. Waters et al., Astron. Astrophys. 315 (1996) L361.
34. K. Demyk, E. Dartois, H. Wiesemeyer, A. P. Jones and L. d'Hendecourt, Astron. Astrophys. 364 (2000) 170.
35. S. Messenger and T. J. Bernatowicz, Meteorit. Planet. Sci. 35 (2000) A109.
36. C. M. O'D. Alexander, L. R. Nittler and F. Tera, Lunar Planet. Sci. XXXII (2001) Abstract #2191.
37. S. Mostefaoui, P. Hoppe, K. K. Marhas and E. Gröner, Meteorit. Planet. Sci. 38 (2003) A99.
38. A. N. Nguyen and E. Zinner, Science 303 (2004) 1496.
39. S. Mostefaoui and P. Hoppe, Meteorit. Planet. Sci. 39 (2004) submitted.
40. K. Nagashima, A. N. Krot and H. Yurimoto, Nature 428 (2004) 921.
41. S. E. Woosley and T. A. Weaver, Astrophys. J. Suppl. 101 (1995) 181.
42. S. Amari, E. Zinner and R. S. Lewis, Astrophys. J. 447 (1995) L147.
43. P. Hoppe, P. Annen, R. Strebel, P. Eberhardt, R. Gallino, M. Lugaro, S. Amari and R. S. Lewis, Astrophys. J. 487 (1997) L101.
44. S. Amari, E. Zinner, R. Gallino, M. Lugaro, O. Straniero and I. Dominguez, In Proc. of Origin of Matter and Evolution of Galaxies 2003 (2004) submitted.